Free Rad. Res., Vol. 22, No. 4, pp. 337-347
Reprints available directly from the publisher
Photocopying permitted by license only

THE USE OF QUANTIFIED MAXIMUM ENTROPY METHODS FOR OPTIMISING INFORMATION FROM ELECTRON PARAMAGNETIC RESONANCE SPECTROSCOPY

B.A. GOODMAN[1], S.M. GLIDEWELL[1] and J. SKILLING[2]

[1]Scottish Crop Research Institute, Invergowrie, Dundee DD2 5DA [2]University of Cambridge, Cavendish Laboratory, Madingley Road, Cambridge, CB3 OHE

(Received January 13th, 1994; accepted July 21st, 1994)

A quantified maximum entropy method is applied to the optimisation of analytical information from EPR spectra of free radicals. Statistically meaningful errors are produced for the positions and intensities of all spectral peaks and considerable improvements in sensitivity compared with conventional spectral enhancement procedures are obtained with measurements of the intensities of spectra of known radicals.

KEY WORDS: Free radical, quantified maximum entropy, spin trap.

INTRODUCTION

Free radicals are of importance in the functioning of all biological systems and have been demonstrated to play vital roles in respiration,[1] metabolism,[2] ageing[3] and senescence[4] in addition to a wide range[5] of disease processes such as atherosclerosis,[6,7] autoimmune diseases,[8] rheumatoid arthritis,[9] emphysema,[10] cancer[11, 12] and Parkinson's disease.[13] Many biologically significant free radicals are very reactive and do not accumulate in tissues to levels that can be detected directly. As a consequence most measurements of free radical activity have been based on assays for the presence of end-products of free radical reactions.[14] Although such an approach has proved to be useful it is not entirely satisfactory because of the multiplicity of reactions which may be initiated by any individual free radical and the difficulty of obtaining dynamic information about reaction processes. Consequently, efforts have been made to use the reactions of free radicals with "spin trap" molecules, which result in the formation of stable radical adducts which can be detected directly by electron paramagnetic resonance (EPR) spectroscopy. This procedure is non-destructive and directly applicable to biological fluids and in some situations to tissue samples. It can, therefore, be used to follow the dynamics of free radical production and the chemical nature of the trapped radicals may be elucidated through analysis of the EPR spectral parameters.[15] In many situations, especially in *in vivo* investigations, the concentrations of adducts are low and the spectra have low signal-to-noise ratios. This severely limits the use of the

All correspondence to Dr. B.A. Goodman, Scottish Crop Research Institute, Invergowrie, Dundee DD2 5DA, Scotland.

technique for analytical measurements, because of the difficulties of accurately determining hyperfine splittings and intensities in poorly resolved spectra.

THEORY

Experimental data differ from their true values for a variety of reasons, some instrumental in origin, others intrinsic to the chemical system, e.g. high viscosity or steric hindrance leading to line broadening in EPR spectra. The conventional methods for spectral enhancement are prone to the creation of artifacts with characteristics resembling genuine peaks and do not provide any statistically-meaningful errors on the derived values. These problems are overcome, at least in part, by the use of a quantified maximum entropy method (MaxEnt). This extends earlier work in maximum entropy spectroscopy[16] by embedding it in probability theory,[17] which uses data D, to infer the "true" underlying function and/or parameters f, along with the probabilistic uncertainty. Here f is the spectrum being sought, and D are the noisy, distorted measurements acquired from the spectrometer. Such inference almost always requires some background hypothesis, H; here H includes the linewidth and lineshape which distort the ideal spectrum, f, into the measured data, D. The formal analysis starts with a *prior* and a *likelihood*.

$\Pr(f|\mathrm{H})$ is the prior, being the intrinsic probability of f. In this work, the prior is defined in terms of the entropy of f, using the standard "$f \log f$" form

$$S\ (f) = \sum(f - m - f \log (f/m))$$

relative to a preassigned model spectrum m which is usually set to be featureless and faint. S is the only functional which has symmetry properties appropriate to reconstructing positive distributions f.[16] With the probabilistic interpretation, maximum entropy just means choosing the most probable solution. The prior defines the theoretical starting point, and is

$$\Pr(f|H) \propto \exp(\alpha \mathrm{S}(f))$$

where the scale parameter α is always assigned its most probable value.

$\Pr(D|f, H)$ is the likelihood, being the probability of finding the particular data, D, as a function of what the true spectrum f might be. All the experimental distortions are incorporated in the likelihood, which encodes the experimental measurements. Deductions are computed through "Bayes' Theorem", which is the identity

$$\Pr(f|D, H) \Pr(D|H) = \Pr(f|H) \Pr(D|f, H)$$

the two sides just being the two factorisations of the joint probability $\Pr(f, D|H)$. The known prior and likelihood factors on the right are used to compute the factors on the left. Specifically,

$$\Pr(D|H) = \int \mathrm{d}f \Pr(f|H) \Pr(D|f, H)$$

whence

$$\Pr(f|D, H) = \Pr(f|H) \Pr(D|f, H)/\Pr(D|H)$$

$\Pr(D|H)$ is a numerical value known as the *evidence*. It describes how well the data could have been predicted in advance. If there is uncertainty about the linewidth or other parameters in the assumptions, H, the evidence can be used to tune these parameters to accord best with the data.

$\Pr(f|D, H)$ is the *inference*, which describes what can be inferred about f, which spectrum is most probable and what are its uncertainties. Usually, this is the aim of probabilistic analysis.

The first step in the analysis of a spectrum by maximum entropy methods is to define a function, called the point spread function (PSF) which represents the distortion imposed on a spectral line. Using an initial estimate of the PSF, the most probable spectrum is calculated as the distribution of intensities which, convolved with the PSF, gives the most probable fit to the observed data. The procedure is iterative; at each step, the trial spectrum is "blurred" by the PSF to give a mock data set; this is compared with the original data and the discrepancies are used to guide the calculation of the next trial spectrum. The calculations are repeated until the result with the maximum evidence is obtained; this is called the MaxEnt result. Some exploration is then made around this optimum, in order to determine the error on each line's position and intensity. This final result has associated with it a value for the evidence, the probability that the observed data result from this series of lines of these intensities convolved with the chosen PSF.

Maximum entropy methods have been used for some time with varying degrees of enthusiasm, for the optimisation of NMR spectra[18-24] in which the spectrum is recorded in the time domain and requires Fourier transformation to the frequency domain before interpretation can begin. EPR spectra are usually still recorded in the frequency domain, and although maximum entropy calculations have been applied,[25,26] the algorithm used in the work reported in this paper additionally has the ability to provide quantitative data as well as visually-enhanced spectra. The present paper describes the use of this approach to provide quantitative information from the EPR spectra of a known, stable free radical, 4-hydroxy-2,2,6,6,-tetramethylpiperidinyloxyl (4-hydroxy-TEMPO), at a series of known concentrations and compares these results with spectra obtained from the same datasets using conventional methods for signal enhancement.

MATERIALS AND METHODS

A 5.81 mM solution of 4-hydroxy-2,2,6,6,tetramethylpiperidinyloxyl free radical (4-hydroxy-TEMPO) (Aldrich) in methanol was made up and diluted 10-fold twice and subsequently 2-fold to give solutions of concentrations ranging from 581 μM to 0.91 μM immediately prior to recording their EPR spectra. These were acquired as first derivatives at ambient temperatures using a Bruker ESP300E computer-controlled X-band spectrometer at a sweep width of 7.5 mT, microwave power 1.0 mW, modulation amplitude 100 mT and modulation frequency 10 kHz. The spectrum consisted of 3 lines separated by the ^{14}N hyperfine coupling and each broadened by the unresolved coupling to the 6 methyl protons. The numerical MaxEnt calculations reported here were carried out with the MemSys5 algorithm, acquired from MaxEnt Solutions Ltd., Isleham, CB7 5QS, UK.

A first estimate of a point spread function (PSF) was made by differentiating a parametric curve constructed of a mixture of Gaussian and Lorentzian lineshapes,

which gave a visual fit to one peak in the cumulant of the observed spectrum of the most concentrated sample (581 μM). This derivative PSF was used to construct a MaxEnt result and to calculate a value for the evidence, which is the probability that the observed data were in accord with that PSF. The linewidth and lineshape were then altered systematically over subsequent runs to maximise the numerical value of the evidence. This optimised PSF was used for the calculations of the spectra of the more dilute samples. It may not always, however, be the case that high signal-to-noise EPR spectra of the spin adduct are available; MaxEnt results were also obtained using a PSF optimised from each spectrum in the manner described above. Calculations were also performed using a composite PSF which comprised the convolution of the MaxEnt result with the PSF for the most concentrated sample. Using this PSF, the MaxEnt result from 4-hydroxy-TEMPO is a single line at the mid-point of the spectrum whose intensity is that of the total spectrum. The use of a composite PSF thus bestows a 3-fold increase in sensitivity for this particular compound.

For comparison, the spectra were also enhanced by a simple 3-point smooth, moving average, polynomial shaped filter and Fourier transform methods as provided in the Bruker standard software package. In order to allow the estimation of experimental error by calculation of means and their standard deviations, eight replicates of each concentration were run in the same total time as for a single scan subsequently treated by MaxEnt.

The 3-point smooth used the algorithm: $y_i = 0.6x_i + 0.2(x_{i-1} + x_{i+1})$ where x_i was the ith original spectrum intensity and y_i the ith resultant spectral intensity. The moving average was calculated according to:

$$y_i = 1/\mathrm{NP} \sum_{j=-(\mathrm{NP}-1)/2}^{+(\mathrm{NP}-1)/2} x_{i+j}$$

where NP was the filter width in data points. The polynomial filter was of the form:

$$y_i = P_0 x_i + \sum_{j=1}^{N} P_1 (x_{i-j} + x_{i+j})$$

where P_k was defined as $[3(3N^2 + 3N\text{-}1\text{-}5k^2)]/[(2N\text{-}1)(2N + 1)(2N + 3)]$, $N = (NP + 1)/2$.

Fourier transform smoothing was carried out by performing a Fourier transform of the spectrum, setting the high frequency portion of the transformed spectrum to zero and then performing a reverse transformation. Having selected an appropriate frequency cutoff for the higher concentration spectra, the same value was used for the spectra from the more dilute solutions.

Of course, these latter methods do not provide quantification from a single scan. Indeed, filters and smoothing usually damage the fit to the data which might otherwise be obtained.

RESULTS AND DISCUSSION

Figures 1 and 2 display data (Figures 1a, 2a) followed by the plots obtained from MaxEnt calculations using respectively a single PSF (Figure 1b) and a 3-peak com-

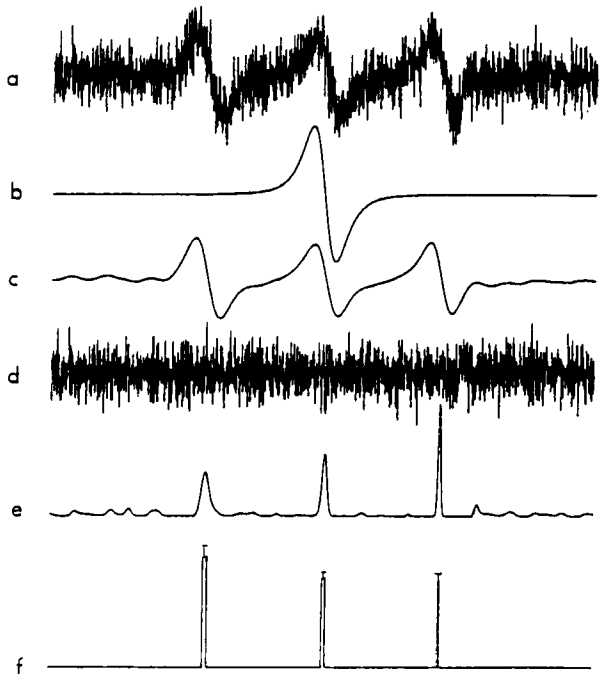

FIGURE 1 MaxEnt results for 14.5 μM 4-hydroxy-TEMPO using a single PSF a) Raw spectrum b) Point Spread Function (PSF) c) Mock Data (convolution of MaxEnt Result with PSF) d) Residual (difference between original spectrum and mock data) e) MaxEnt result f) Spike plot with errors (see text for explanation).

posite PSF (Figure 2b) as described above. The mock data (Figures 1c, 2c), are convolutions of the PSF with the MaxEnt result and picture the 'noise-free' spectra. Subtraction of the mock data from the original spectrum gives the residuals which are essentially noise (Figures 1d, 2d). Were it otherwise, that would suggest a miscalibration or other systematic error. As it is, the MaxEnt results are seen to be at least plausible. The MaxEnt results are in Figures 1e, 2e and the spike plot with errors in Figures 1f, 2f. Spike plots are displays of the MaxEnt result in which each statistically significant peak is plotted at its average position as a spike whose height represents peak area. This avoids the interpretative difficulty of visually relating peaks of similar areas, but differing heights and widths. Figures 1f and 2f are "spike plots with errors" where height still represents area, but where width represents positional uncertainty (plus/minus one standard deviation).

In addition to calculating the position of the lines and the errors on their positions, the MaxEnt package also calculates the intensities and their 95% probability limits which are represented by vertical bars on the spike plots with errors. It thus represents a method for estimating the concentrations of free radicals in extremely dilute solutions which appear to consist almost entirely of noise (Figure 3a) although it should be noted (Figure 3b) that very high uncertainties are associated with the values obtained from such very poor signal-to-noise spectra. At the margin, it is

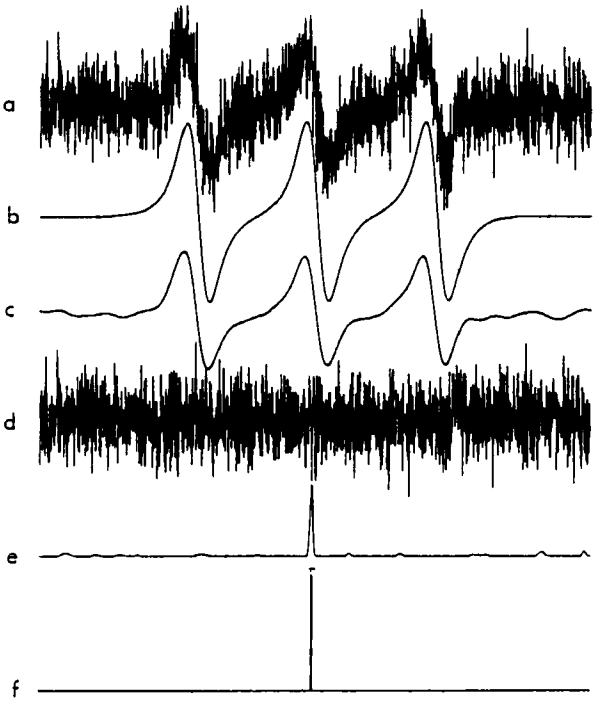

FIGURE 2 MaxEnt results for 14.5 μM 4-hydroxy-TEMPO using a composite PSF a) Raw spectrum b) Point Spread Function (PSF) c) Mock Data (convolution of MaxEnt Result with PSF) d) Residual (difference between original spectrum and mock data) e) MaxEnt result f) Spike plot with errors (see text for explanation).

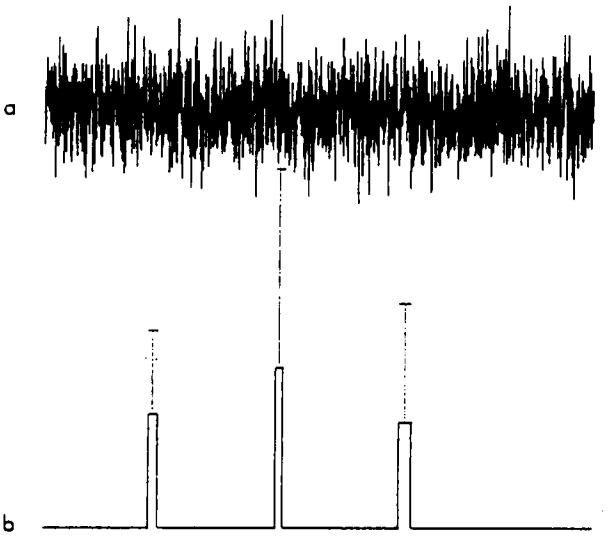

FIGURE 3 MaxEnt results for 0.91 μM 4-hydroxy-TEMPO a) Raw spectrum b) Spike plot with errors.

necessary to use a PSF derived elsewhere, because excessively noisy data do not contain enough information to estimate the PSF as well as the spectrum.

The intensities calculated from a series of solutions of different concentrations are plotted against their concentrations in Figure 4 and show reasonable agreement within experimental error with the ideal straight line of gradient 1 for both single and composite PSFs (the latter not shown as the two datasets overlap). Figure 4 also shows the plots obtained from peak to peak measurements made on the original

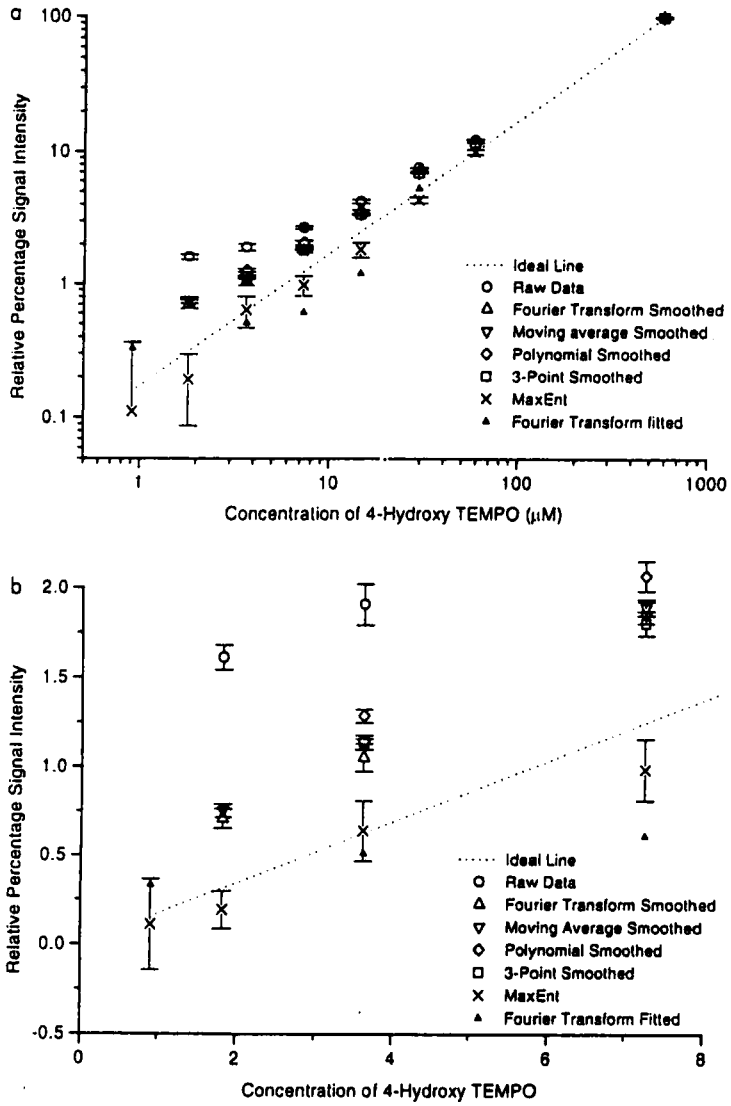

FIGURE 4 Comparison of different spectral enhancement techniques a) Plot of spectrally derived concentrations against actual concentrations of 4-hydroxy-TEMPO b) Expansion of low concentration portion of Fig. 4(a).

and Fourier Transform enhanced spectra as well spectra smoothed by three other commonly used methods. In order to obtain estimates of the measurement errors associated with the various smoothing techniques, it was necessary to run repeated scans and then measure means and standard deviations of the replicates. To make a fair comparison, bearing in mind the relative instability of many biologically-derived radicals, these were run in the same total time as a single scan for MaxEnt analysis. It is nonetheless important to realise that errors always have to be estimated from the data to hand. Dividing the available acquisition time into N parts, to acquire N subsidiary spectra, just increases the individual noise levels by a factor of $N^{1/2}$ without gleaning any new relevant information. If spectrum features can still be detected from the individual acquisitions, then all well and good, and the variability of a feature will give a crude but pessimistically wide guess about the accuracy of its estimation. (In the limit of large N, the individual spectra will be so noisy that no feature would be detectable, so the variability could not be estimated at all.) These points are borne out by the results obtained from this approach (Figure 4) which show high precision but low accuracy and inability to cope with the lowest concentration. Unless there is reason to expect time variations in the sample, it is always better to apply proper statistical inference once to the combined data taken as a whole. In this paper, we analyse a sub-divided dataset purely in order to make comparisons; we recommend against the practice as a normal procedure.

Figure 4 shows that by all of the spectral smoothing methods, overestimates of the free radical concentrations were obtained at all values, and the error bars representing one standard deviation did not overlap the theoretical line in all save the 58.1 μM solution (the 581 μM solution is constrained to fit). In contrast, the spectral intensities derived from MaxEnt analysis of the experimental data were much closer to the expected values. In addition, it was also possible to obtain spectral intensities by MaxEnt analysis at lower concentrations than was possible by the use of smoothing methods on spectra acquired over the same period of time. For the 4-hydroxy TEMPO, the intensity of the MaxEnt result using a three-peak PSF was three times greater than that obtained with a single peak PSF, and with more complex PSFs for multiline spectra, even greater increases in sensitivity could be obtained.

The spectra obtained by Fourier transform enhancement, which are shown in Figure 5, were broadly comparable with those produced by the MaxEnt package, except for very poor quality spectra (see Figure 5d). These latter could be improved, in appearance although not in closeness of fit to the ideal line (see Figure 4), by subsequent curve fitting, using the Marquardt-Levenberg non-linear least-squares algorithm, of their integrals to three Lorentzian lineshapes. This procedure uses the prior expectation of three lines in contrast to MaxEnt which uses the lineshape as its prior knowledge. The results obtained from treating a spectrum with fairly good signal-to-noise, with a simple 3-point smooth, moving average and 3rd order polynomial filtering are presented in Figure 6 for comparison.

These measurements demonstrate the effectiveness of quantified maximum entropy as a means of obtaining meaningful estimates of *quantitative* intensity data and hyperfine splittings from a single EPR spectrum. This is of particular importance when dealing with biological systems in which free radicals are often present at low concentrations, and of limited lifetimes, but whose absolute or relative values are of significance. Although in the results presented here, a PSF derived from concentrated solutions of a known radical species was used to calculate the amount

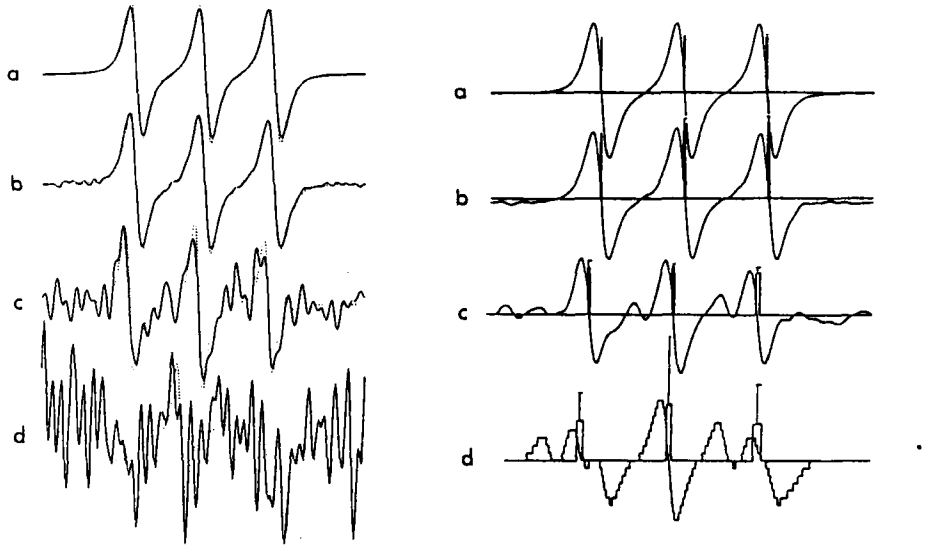

FIGURE 5 Comparison of Fourier Transform spectral enhancement (left - dotted line shows fitted FT enhanced result) and MaxEnt Mock Data (right) for a range of 4-hydroxy-TEMPO concentrations a) 581 μM b) 58.1 μM c) 7.25 μM d) 0.91 μM.

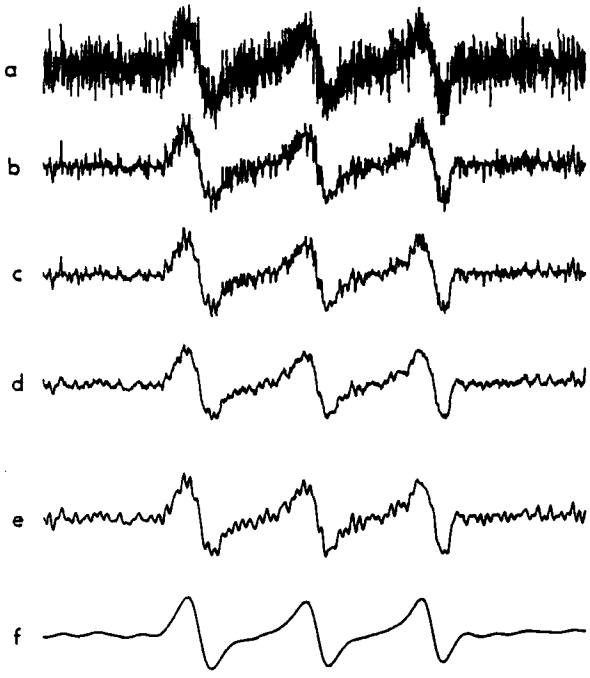

FIGURE 6 Comparison of different spectral enhancement techniques on spectrum of 58.1μM 4-hydroxy-TEMPO a) Raw spectrum b) 3rd order polynomial filter 10 timesc) 3-point smooth 10 times d) Moving average filter width 15 data pointse) Fourier Transform enhanced f) Mock data from MaxEnt.

of that species present in dilute solutions, the results obtained were in fact not markedly different from those obtained by using a PSF optimised for each spectrum at even the lowest concentrations. A major advantage of quantified maximum entropy over other methods of data enhancement is its ability to obtain *quantitative data* with associated estimates of error from a single spectrum as it can calculate the *amount* of a given radical species in very dilute solutions. In order to obtain error estimates by other methods, the spectrum must be run several times and means and standard deviations of intensities calculated. This is not always conducive to consistent results when dealing with biological samples available in small amounts or of limited stability.

The measurements described here were all performed on solutions containing only one spin species. Extension to systems containing more than one type of free radical is straightforward if the peaks of all components can be described by a single PSF. Analyses become extremely difficult, however, when this assumption is no longer valid and where different spin species give rise to different lineshapes. In such situations the different parts of the spectrum need to be treated separately; this does not affect the ability of MaxEnt to 'pick out' a selected spin species as in this case and to calculate the intensity and position of its lines. However, when molecular motion is restricted, and spectra become anisotropic, the lineshapes can no longer be extrapolated from one peak to another; at present the MaxEnt approach described in this paper is not applicable to such situations.

CONCLUSIONS

Quantified maximum entropy based software provides a dramatic increase in sensitivity for reconstructing EPR spectra and measuring the concentrations of specific multipeak components. As a useful advance, it provides statistically meaningful errors associated with such quantitative measurements. It thus represents a powerful technique for use in the study of biological free radicals and may prove to be of particular value in the measurement of the concentration of radical adducts which are produced by the reactions of chemical "spin traps" with unstable biological radicals.

Acknowledgement

This work was funded by the Scottish Office Agriculture and Fisheries Department (SOAFD).

References

1. H. Nohl (1994) Generation of Superoxide Radicals as By-Product of Cellular Respiration. *Annales de Biologie Clinique*, **52**, 199–204.
2. D.C. Liebler (1993) The Role of Metabolism in the Antioxidant Function of Vitamin E. *Critical Reviews in Toxicology*, **23**, 147–169.
3. R.S. Sohal (1993) The Free Radical Hypothesis of Aging - An Appraisal of the Current Status. *Aging - Clinical and Experimental Research*, **5**, 3–17.
4. K.T.I. Suzuki (1993) Origin of Senescence - A Review. *Hormone Research*, **39**, 5–8.
5. J.P.T.I. Kehrer (1993) Free Radicals as Mediators of Tissue Injury and Disease.*Critical Reviews in Toxicology*, **23**, 21–48.
6. B. Halliwell (1993) The Role of Oxygen Radicals in Human Disease, With Particular Reference to the Vascular System. *Haemostasis*, **23**, 118–126.

7. M.A. Weiner, S.B. Paige and S.R. Bailey (1993) The Effects of Iron, Free Radicals and Antioxidants on the Development of Atherosclerosis. *Clinical Research*, **41**, 782.
8. A. Rabinovitch (1992) Free Radicals as Mediators of Pancreatic Islet Beta-Cell Injury in Autoimmune Diabetes. *Journal of Laboratory and Clinical Medicine*, **119**, 455–456.
9. K. Bernacka, S. Sierakowski, P.A. Klimiuk and J. Chwiecko (1992) Concentration of Malondialdehyde in the Serum of Patients with Rheumatoid Arthritis. *Folia Histochemica et Cytobiologica*, **30**, 203–204.
10. H. Kanazawa, N. Kurihara, K. Hirata, S. Fujimoto and T. Takeda (1992) The Role of Free Radicals and Neutrophil Elastase in Development of Pulmonary Emphysema. *Internal Medicine*, **31**, 857–860.
11. A.S. Salim (1993) Oxygen-Derived Free Radicals - Implications for Gastrointestinal Cancer (Review). *International Journal of Oncology*, **2**, 309–319.
12. S.C. Sahu (1992) Dietary Iron and Cancer - A Review. *Environmental Carcinogenesis & Ecotoxicology Reviews - Part C of Journal of Environmental Science and Health*, **10**, 205–237.
13. J.D. Adams and I.N. Odunze (1991) Oxygen Free Radicals and Parkinson's Disease. *Free Radical Biology and Medicine*, **10**, 161–169.
14. R.H. Burdon and P.H. van Knippenberg (Eds) (1991) *Laboratory Techniques in Biochemistry and Molecular Biology Volume 22, Techniques in Free Radical Research*, Elsevier, London.
15. G. Buettner (1987) Spin Trapping: ESR Parameters of Spin Adducts. *Free Radicals in Biology and Medicine*, **3**, 259–303.
16. E.D. Laue, J. Skilling, J. Staunton, S. Sibisi and R.G. Brereton (1985) Maximum Entropy Method in Nuclear Magnetic Resonance Spectroscopy. *Journal of Magnetic Resonance*, **62**, 437–452.
17. R.T. Cox (1946) Probability, Frequency and Reasonable Expectation. *American Journal of Physics*, **14**, 1–13.
18. J. Skilling (1989) Classic Maximum Entropy. In *Maximum Entropy and Bayesian Methods, Cambridge, 1988*, (ed. J. Skilling), Kluwer Academic Publishers, Dordrecht, pp. 45–52.
19. J.F. Martin (1985) The Maximum Entropy Method in NMR. *Journal of Magnetic Resonance*, **65**, 291–297.
20. J.K. Kaupinnen, D.J. Moffatt and H.H. Mantsch (1992) Nonlinearity of the Maximum Entropy Method in Resolution Enhancement. *Canadian Journal of Chemistry*, **70**, 2887–2894.
21. R.E. Hoffman and G.C. Levy (1991) NMR Data Processing and Evaluation. *Progress in NMR Spectroscopy*, **23**, 211–258.
22. J.J. Kotyk, N.G. Hoffman, W.C. Hutton, G.L. Bretthorst and J.J.H. Ackermann (1992) Comparison of Fourier and Bayesian Analysis of NMR Signals. I. Well-Separated Resonances (The Single Frequency Case). *Journal of Magnetic Resonance*, **98**, 483–500.
23. J.A. Jones and P.J. Hore (1991) The Maximum Entropy Method and Fourier Transformation Compared. *Journal of Magnetic Resonance*, **92**, 276–292.
24. J.A. Jones and P.J. Hore (1991) The Maximum Entropy Method. Appearance and Reality. *Journal of Magnetic Resonance*, **92**, 363–371.
25. R.A. Jackson (1987) Application of the Maximum Entropy Method to the Analysis of Electron Spin Resonance Spectra. *Journal of Magnetic Resonance*, **75**, 174–178.
26. R.A. Jackson (1994) Objective Analysis of EPR Spectra by Computer Methods. *Journal of the Chemical Society, Perkin Transactions 2*, 1991–1994.

Accepted by V. Darley-Usmar